



On the multiaxial fatigue assessment of thin welded joints: a preliminary investigation

L. Susmel

Department of Civil and Structural Engineering, The University of Sheffield, Mappin Street, Sheffield, S1 3JD, UK
l.susmel@sheffield.ac.uk

H. Askes

Department of Civil and Structural Engineering, The University of Sheffield, Mappin Street, Sheffield, S1 3JD, UK
h.asks@sheffield.ac.uk

ABSTRACT. The present paper is concerned with the use of the Modified Wöhler Curve Method to estimate fatigue lifetime of thin welded joints of both steel and aluminium subjected to in-phase and out-of-phase multiaxial fatigue loading. The most important peculiarity of the above multiaxial fatigue criterion is that it can be applied by performing the stress analysis in terms of both nominal and local quantities, where in the latter case the relevant stress state at the assumed critical locations can be estimated according to either the reference radius concept or the Theory of Critical Distances. The accuracy and reliability of our multiaxial fatigue criterion was systematically checked through several experimental results taken from the literature and generated by testing, under in-phase and out-of-phase biaxial loading, welded joints of both steel and aluminium having thickness of the main tube lower than 5 mm.

SOMMARIO. Scopo del presente lavoro è quello di investigare l'accuratezza del Criterio delle Curve di Wöhler Modificate nel prevedere la resistenza a fatica multiaassiale di giunzioni saldate sottili. Una delle più importanti peculiarità del Criterio delle Curve di Wöhler Modificate risiede nel fatto che il danneggiamento a fatica può essere direttamente stimato eseguendo l'analisi tensionale in termini sia di tensioni nominali che di tensioni locali, ovvero in accordo sia con l'approccio del raggio fittizio che con la Teoria delle Distanze Critiche. L'accuratezza del Criterio delle Curve di Wöhler modificate è stata infine investigata rianalizzando una serie di risultati sperimentali di letteratura generati testando provini saldati cilindrici sia in acciaio che in alluminio sollecitati da carichi biassiali di fatica sia in fase che fuori fase, dove tali provini erano caratterizzati da uno spessore del tubo principale inferiore a 5mm.

KEYWORDS. Thin welded joints; Multiaxial fatigue; Modified Wöhler Curve Method.

INTRODUCTION

The fatigue design curves stated by the available standard codes [1, 2] and recommendations [3] were determined by statistically re-analysing a large number of experimental results generated in different laboratories by testing samples not only having different geometries, but also manufactured by adopting different welding technologies. The common feature of the above laboratory specimens was that they were characterised by a relatively large thickness (in general, larger than 5 mm), so that, strictly speaking, the available design curves can efficiently be used to design against fatigue solely thick and stiff welded structures.



In recent years, thanks also to the development and optimisation of new welding technologies, much progress has been made in order to set up new welding processes suitable for efficiently and accurately manufacturing thin welded connections of both steel and aluminium. Owing to their specific structural features, nowadays thin welded joints are widely used in different industrial sectors and, amongst them, certainly the automotive industry deserves to be mentioned. In this scenario, aim of the present paper is investigating the accuracy of the so-called Modified Wöhler Curve Method (MWCM) [4] in estimating lifetime of thin welded joints subjected to in-phase and out-phase multiaxial fatigue loading.

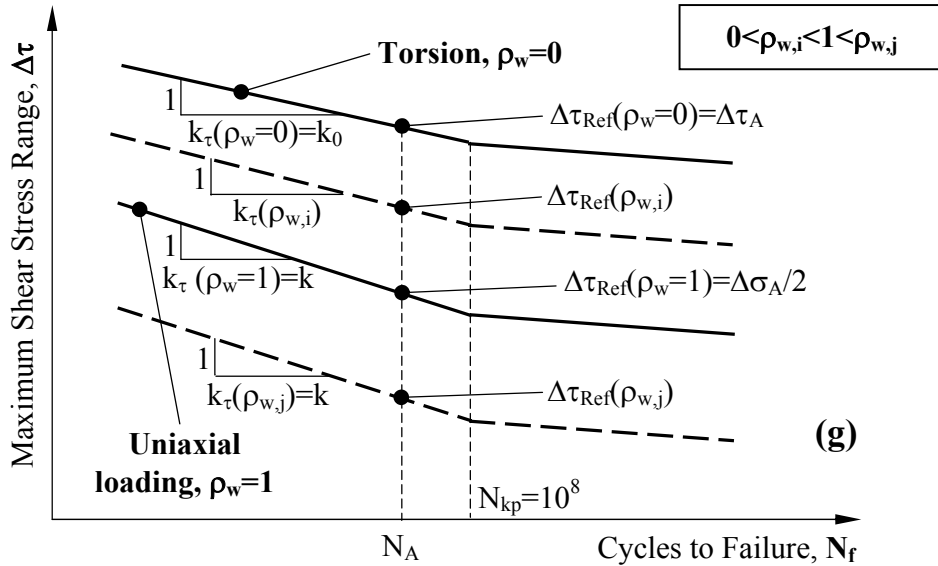


Figure 1: Modified Wöhler diagram for welded joints.

THE MWCM IN MULTIAXIAL FATIGUE ASSESMENT OF WELDED JOINTS

The MWCM is a critical plane approach which estimates multiaxial fatigue damage in welded joints through the maximum shear stress range, $\Delta\tau$, as well as through the range, $\Delta\sigma_n$, of the stress perpendicular to the critical plane. According to the fatigue damage model the MWCM is based on [4, 5], the critical plane is defined as that material plane experiencing the maximum shear stress range, such a stress quantity being determined according to the Maximum Variance Method [6].

From a practical point of view, the combined effects of both $\Delta\tau$ and $\Delta\sigma_n$ are taken into account simultaneously through the following stress index [4, 7]:

$$\rho_w = \frac{\Delta\sigma_n}{\Delta\tau} \quad (1)$$

The most relevant aspect of the above stress ratio is that it is fully sensitive to the degree of multiaxiality and non-proportionality of the assessed stress state: for instance, ρ_w is equal to unity and to zero under pure axial and pure torsional fatigue loading, respectively, whereas, given the ratio between the amplitudes of the applied stress components, its value changes as the non-proportionality level of the applied load history varies [4].

Turning back to the MWCM, the way it estimates fatigue damage under multiaxial fatigue loading is schematically shown in the modified Wöhler diagram reported in Fig. 1. The above log-log diagram plots the shear stress range relative to the critical plane, $\Delta\tau$, against the number of cycles to failure, N_f . By performing a systematic reanalysis based on numerous experimental data [4, 7, 8], it was proven that, as ratio ρ_w varies, different fatigue curves are obtained (Fig. 1). In particular, it was observed that fatigue damage tends to increase as ρ_w increases: this results in the fact that the corresponding fatigue curve tends to shift downward in the above diagram with increasing of ρ_w (Fig. 1). According to the classical log-log schematisation used to summarise fatigue data, the position and the negative inverse slope of any Modified Wöhler curve can unambiguously be defined through the following linear relationships [4, 7, 8]:



$$k_{\tau}(\rho_w) = (k - k_0) \cdot \rho_w + k_0 \quad (2)$$

$$\Delta\tau_{\text{Ref}}(\rho_w) = \left(\frac{\Delta\sigma_{\Lambda} - \Delta\tau_{\Lambda}}{2} \right) \cdot \rho_w + \Delta\tau_{\Lambda} \quad (3)$$

where k and k_0 are the negative inverse slopes of the uniaxial and torsional fatigue curve, respectively, whereas $\Delta\sigma_{\Lambda}$ and $\Delta\tau_{\Lambda}$ are the ranges of the corresponding reference stresses extrapolated at N_{Λ} cycles to failure (see Fig. 1).

Another important aspect which deserves to be discussed in great detail is the fact that the reference shear stress range to be used to estimate multiaxial fatigue damage, i.e. Eq. (3), is assumed to be constant and equal to $\Delta\tau_{\text{Ref}}(\rho_{\text{lim}})$ for ρ_w larger than limit value ρ_{lim} [4]. This correction, which plays a fundamental role in the overall accuracy of the MWCM, was introduced in light of the fact that, under large values of ratio ρ_w , the predictions made by the MWCM were seen to become too conservative [9]. According to the experimental results due to Kaufman and Topper [10], such a high degree of conservatism was ascribed to the fact that, when micro/meso cracks are fully open, an increase of the normal mean stress does not result in a further increase of fatigue damage. Therefore, by taking full advantage of the intrinsic mathematical limit of Eq. (3) [4], ρ_{lim} takes on the following value:

$$\rho_{w,\text{lim}} = \frac{\Delta\tau_{\Lambda}}{2\Delta\tau_{\Lambda} - \Delta\sigma_{\Lambda}} \quad (4)$$

In a similar way, also the k_{τ} vs. ρ_w relationship, Eq. (2), is recommended to be corrected as follows:

$$k_{\tau}(\rho_w) = [k - k_0] \cdot \rho_w + k_0 \quad \text{for } \rho_w \leq 1 \text{ and } N_f \leq N_{k_p} \quad (5)$$

$$k_{\tau}(\rho_w) \equiv k \quad \text{for } \rho_w > 1 \text{ and } N_f \leq N_{k_p} \quad (6)$$

N_{k_p} being the number of cycles to failure that defines the position of the knee point (Fig. 1). In the high/giga cycle fatigue regime, that is, for $N_f > N_{k_p}$ instead, the slope of the Modified Wöhler Curves is suggested as being taken invariably equal to 22 [24] independently from the actual value of the ρ_w ratio. As to the position of the knee point, it is worth observing here that, under axial loading, the International Institute of Welding (IIW) [3] recommends to take the knee point at $N_{k_p} = 10^7$ cycles to failure, on the contrary, under torsional loading, at $N_{k_p} = 10^8$ cycles to failure. Since the MWCM is a shear stress based criterion, the knee point can then be taken at 10^8 cycles to failure independently from the actual value of ratio ρ_w [12].

Turning back to the way the negative inverse slope, $k_{\tau}(\rho_w)$, varies as ρ_w ratio increases, the hypothesis is formed that the negative inverse slope is constant and invariably equal to k for $\rho_w > 1$, Eq. (6). The assumption is derived from the experimental evidence that, in general, as far as welded joints are concerned, the slope of the Modified Wöhler curves is never seen to be lower than the one of the uniaxial fatigue curve [4], this holding true independently from the degree of multiaxiality and non-proportionality of the applied load history.

To conclude, as suggested by the modified Wöhler diagram sketched in Fig. 1, as soon as the appropriate Modified Wöhler Curve estimated through Eqs (2) to (6) is known for the specific value of ρ_w damaging the critical plane, the number of cycles to failure can directly be calculated as follows:

$$N_{f,c} = N_{\Lambda} \cdot \left[\frac{\Delta\tau_{\text{Ref}}(\rho_w)}{\Delta\tau} \right]^{k_{\tau}(\rho_w)} \quad (7)$$

STRESS AND STRENGTH ANALYSIS

By nature, the MWCM can be applied by performing the stress analysis according to different strategies [4, 13], i.e., nominal (and hot-spot) stresses [7, 8], the reference radius concept [12] and the Theory of Critical Distances [14, 15].



In more detail, as soon as the nominal stress components damaging the welded connection being assessed are known, the MWCM can directly be applied by calibrating it through the design curves supplied by the proper standard codes [1-3], provided that, the designed weldments work in the as-welded condition. On the contrary, if welded joints are stress relieved, such connections are suggested as being designed against fatigue by multiplying the reference shear stress range of the adopted modified Wöhler curve, $\Delta\tau_{\text{Ref}}(\rho_w)$ – Eq. (3), by a suitable enhancement factor, $f(R_{\text{CP}})$, that is [3, 12, 16]:

$$\Delta\tau_{\text{Ref}}(\rho_w) \cdot f(R_{\text{CP}}) = (a \cdot \rho_w + b) \cdot f(R_{\text{CP}}) \quad (8)$$

where enhancement factor $f(R_{\text{CP}})$ is assumed to depend on the following load ratio [4]:

$$R_{\text{CP}} = \frac{\sigma_{n,\text{min}}}{\sigma_{n,\text{max}}}, \quad (9)$$

$\sigma_{n,\text{max}}$ and $\sigma_{n,\text{min}}$ being the maximum and minimum value of the stress perpendicular to the critical plane, respectively. According the above considerations, the rules recommended by Sonsino in Ref. [16] can directly be extended to those situations involving multiaxial fatigue loadings as follows:

$$\begin{aligned} f(R_{\text{CP}}) &= 1.32 && \text{for } R_{\text{CP}} < -1 \\ f(R_{\text{CP}}) &= -0.22 \times R_{\text{CP}} + 1.1 && \text{for } -1 \leq R_{\text{CP}} \leq 0 \\ f(R_{\text{CP}}) &= -0.2 \times R_{\text{CP}} + 1.1 && \text{for } 0 < R_{\text{CP}} \leq 0.5 \\ f(R_{\text{CP}}) &= 1 && \text{for } R_{\text{CP}} > 0.5 \end{aligned} \quad (10)$$

for steel welded joints and

$$\begin{aligned} f(R_{\text{CP}}) &= 1.88 && \text{for } R_{\text{CP}} < -1 \\ f(R_{\text{CP}}) &= -0.55 \times R_{\text{CP}} + 1.33 && \text{for } -1 \leq R_{\text{CP}} \leq 0 \\ f(R_{\text{CP}}) &= -0.66 \times R_{\text{CP}} + 1.33 && \text{for } 0 < R_{\text{CP}} \leq 0.5 \\ f(R_{\text{CP}}) &= 1 && \text{for } R_{\text{CP}} > 0.5 \end{aligned} \quad (11)$$

for aluminium welded joints.

The most modern fatigue design method which is recommended by the IIW [3, 16] for the design of thin welded joints against fatigue is that based on the use of a fictitious radius: according to such an approach, the relevant stress states in welded joints having thickness of the main plate lower than 5 mm have to be determined by rounding the profile of either the weld toe or root with a fillet having radius, r_{ref} , equal to 0.05 mm. As soon as the stress state determined at the critical location according to the above strategy is known, lifetime under uniaxial fatigue loading can directly be estimated through a design curve having reference stress range, $\Delta\sigma_A$, calculated, according to the maximum principal stress criterion, at $N_A = 2 \cdot 10^6$ cycles to failure equal to 630 MPa for steel weldments and to 180 MPa for aluminium joints, such reference ranges being estimated for a probability of survival, P_s , equal to 97.7% and evaluated, to simulate the damaging effect of high tensile residual stresses, at a load ratio, R , equal to 0.5. Further, the above uniaxial reference fatigue curve has its knee point, N_{kp} , at 10^7 cycles to failure and its negative inverse slope, k , is equal to 3 for $N_f \leq N_{\text{kp}}$ and to 22 for $N_f > N_{\text{kp}}$ [3, 16], such a schematisation applying to both steel and aluminium thin welded joints. On the contrary, as far as torsional cyclic loadings are concerned, the design curve, again determined according to the maximum principal stress hypothesis, suggested by Sonsino [16] as being used to perform the fatigue assessment according to the $r_{\text{ref}} = 0.05$ mm concept has reference shear stress range, $\Delta\tau_A$, at $N_A = 2 \cdot 10^6$ cycles to failure equal to 250 MPa and to 90 MPa for steel and aluminium welded joints, respectively. Further, the negative inverse slope, k_0 , is equal to 5 for $N_f \leq N_{\text{kp}}$ and to 22 for $N_f > N_{\text{kp}}$, where N_{kp} is recommended to be taken at 10^8 cycles to failure [16].

Another important aspect is the fact that the fatigue curves as defined in the previous paragraphs are suggested to be used to design against fatigue solely “stiff” welded joints. On the contrary, when welded connections behave like “flexible” structures, the negative inverse slope of the corresponding design curve is seen to increase from 3 up to 5 under uniaxial fatigue loading and from 5 up to 7 under torsional loading [17].

Another important issue is that the uniaxial and torsional design fatigue curves as defined above can safely be used to calibrate the constants in the MWCM’s governing equations solely when our criterion is meant to be used to design



welded joints working in the as-welded condition. On the contrary, to correctly account for the effect of superimposed static stresses in stress relieved welded connections, the stress range at N_A cycles to failure of any modified Wöhler curve is suggested as being corrected through enhancement factor $f(R_{CP})$ - Eq. (9), such a factor being again calculated according to definitions (10) and (11) [12].

In recent years, much progress has been made to validate against experimental data an alternative local design methodology whose formalisation takes full advantage of the Theory of Critical Distances (TCD) applied in the form of the classical Point Method (PM) [4, 14, 15]. In more detail, our approach estimates fatigue damage in welded connections subjected to in-service time-variable loadings by directly post-processing the linear-elastic stress fields acting on the material in the vicinity of the assumed crack initiation sites, both weld toes and weld roots being modelled as sharp notches. The stress state to be used to determine the necessary stress quantities relative the critical plane has to be determined, along the bisector (i.e., along the focus path), at distance from the weld toe apex (or the weld root apex) equal to $M \cdot D_V$, such a critical distance being equal to 0.5 mm for steel welded joints [14] and to 0.075 mm for aluminium welded connections [15].

As soon as the time-variable stress state at the critical location is known, the range of the maximum shear stress, $\Delta\tau$, and the range of the stress perpendicular to the critical plane, $\Delta\sigma_n$, can directly be determined by taking full advantage of the Maximum Variance Method [6]. Subsequently, the calculated value for ratio ρ_w , Eq. (1), allows the negative inverse slope, $k_\tau(\rho_w)$, and the reference shear stress range, $\Delta\tau_{Ref}(\rho_w)$, of the appropriate modified Wöhler curve to be estimated from the calibration functions reported below. In more detail, for steel welded joints $k_\tau(\rho_w)$ takes on the following values [14]:

$$k_\tau(\rho_w) = -2 \cdot \rho_w + 5 \quad \text{for } \rho_w \leq 1 \quad (12)$$

$$k_\tau(\rho_w) = 3 \quad \text{for } \rho_w > 1 \quad (13)$$

whereas $\Delta\tau_{Ref}(\rho_w)$ at $N_A=5 \cdot 10^6$ cycles to failure can be estimated as [18]:

$$\Delta\tau_{Ref}(\rho_w) = -32 \cdot \rho_w + 96 \text{ [MPa]} \quad \text{for } \rho_w \leq 2 \quad (14)$$

$$\Delta\tau_{Ref}(\rho_w) = 32 \text{ [MPa]} \quad \text{for } \rho_w > 2 \quad (15)$$

for a Probability of Survival, P_S , equal to 50%, and as [17]:

$$\Delta\tau_{A,Ref}(\rho_w) = -24 \cdot \rho_w + 67 \text{ [MPa]} \quad \text{for } \rho_w \leq 2 \quad (16)$$

$$\Delta\tau_{A,Ref}(\rho_w) = 19 \text{ [MPa]} \quad \text{for } \rho_w > 2 \quad (17)$$

for $P_S=97.7\%$. On the contrary, as far as aluminium welded connections are concerned, the constants in the MWCM's governing equations are suggested as being estimated as follows (where $N_A=5 \cdot 10^6$ cycles to failure) [15]:

$$k_\tau(\rho_w) = -0.5 \cdot \rho_w + 5 \quad \text{for } \rho_w \leq 4 \quad (18)$$

$$k_\tau(\rho_w) = 3 \quad \text{for } \rho_w > 4 \quad (19)$$

$$\Delta\tau_{Ref}(\rho_w) = -1.3 \cdot \rho_w + 33.6 \text{ [MPa]} \quad \text{for } \rho_w \leq 4 \quad (20)$$

$$\Delta\tau_{Ref}(\rho_w) = 28.4 \text{ [MPa]} \quad \text{for } \rho_w > 4 \quad (21)$$

for $P_S=50\%$, and

$$\Delta\tau_{Ref}(\rho_w) = -5 \cdot \rho_w + 28 \text{ [MPa]} \quad \text{for } \rho_w \leq 4 \quad (22)$$

$$\Delta\tau_{Ref}(\rho_w) = 8 \text{ [MPa]} \quad \text{for } \rho_w > 4 \quad (23)$$

for $P_S=97.7\%$.

To conclude, it is worth observing that, strictly speaking, the $\Delta\tau_{Ref}$ vs. ρ_w relationships summarised above are valid solely to design welded joints working in the as-welded condition [14, 15]. On the contrary, if the welded joints being assessed are stress relieved, the presence of non-zero mean stresses is recommended to be taken into account through a procedure similar to the one stated by Eurocode 3 [1], that is, by making use of an effective shear stress range calculated by adding

the tensile part to 60% of the compressive portion of the shear stress range [4, 15]. Accordingly, a suitable shear stress enhancement factor, $f(\tau)$, can directly be calculated as follows:

$$f(\tau) = 1 \quad \text{for } (\tau_m - \tau_a) \geq 0 \quad (24)$$

$$f(\tau) = \frac{2\tau_a}{|\tau_m + \tau_a| + 0.6|\tau_m - \tau_a|} \quad \text{for } (\tau_m - \tau_a) < 0 \quad (25)$$

where τ_m and τ_a are the mean value and the amplitude, respectively, of the shear stress relative to the critical plane [19]. As to the above correction, it is worth observing here that it can safely be used to design stress relieved welded joints made not only of steel (as recommended by Eurocode 3 [1]), but also of aluminium, since, in the latter case, the use of enhancement factor $f(\tau)$ results in corrections that are characterised by a level of conservatism larger than the one obtained by adopting the enhancement factor values suggested by Sonsino [16].

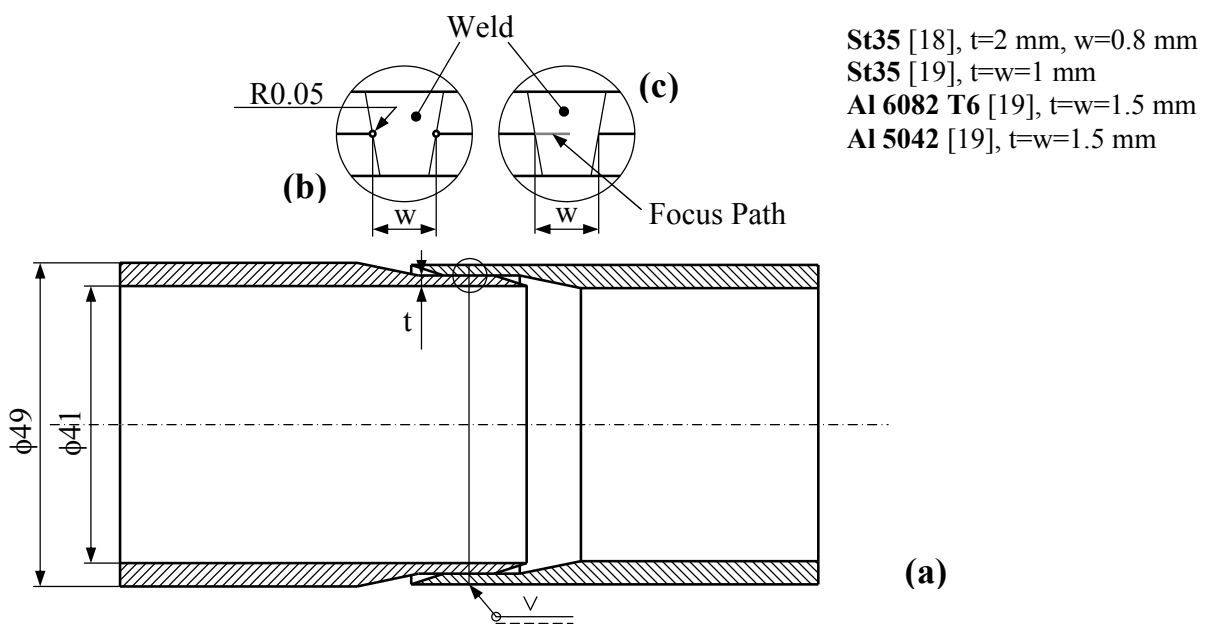


Figure 2: Steel and aluminium laser beam welded joints tested at LBF, Darmstadt, Germany [18, 19].

VALIDATION BY EXPERIMENTAL RESULTS

By performing a systematic bibliographical investigation, a number of data sets were selected from the technical literature, the considered experimental results being generated by testing cylindrical welded samples of both steel and aluminium having thickness of the main tube varying in the range 1-3.2 mm.

Fig. 2a shows the geometry of the steel and aluminium laser beam welded joints tested at Fraunhofer-Institute for Structural Durability and System Reliability LBF, Darmstadt, Germany [18, 19]. Razmjoo [20] instead tested, under combined tension and torsion, fillet welded tube-to-flange specimens having thickness of the main tube equal to 3.2 mm (Fig. 3), a manual metal arc process being adopted to manufacture the welded samples. Finally, the set of experimental results generated by Costa et al. [21] by testing, under combined bending and torsion, the tubular samples of Al 6060-T6 sketched in Fig. 4 was also considered in the validation exercise discussed in what follows.

Initially, attention was focussed on the accuracy of the MWCM in predicting multiaxial fatigue lifetime of thin welded joints when our approach is applied in terms of nominal stresses. The experimental, N_{f_i} , vs. estimated, $N_{f_{i,e}}$, number of cycles to failure diagrams reported in Fig. 5a show that, by calibrating the MWCM through the appropriate FAT curves recalculated for a Probability of Survival, P_s , equal to 50%, the use of our criterion resulted in estimates falling within the axial and torsional reference scatter bands. In the charts of Fig. 5 the continuous and dashed straight lines delimit the



standard uniaxial and torsional fatigue scatter bands, respectively, the plotted scatter bands being recalculated from the reference value of 1.8 suggested by Haibach and determined by considering fatigue curves characterised by a P_S value equal to 2.3% and 97.7%, respectively [29].

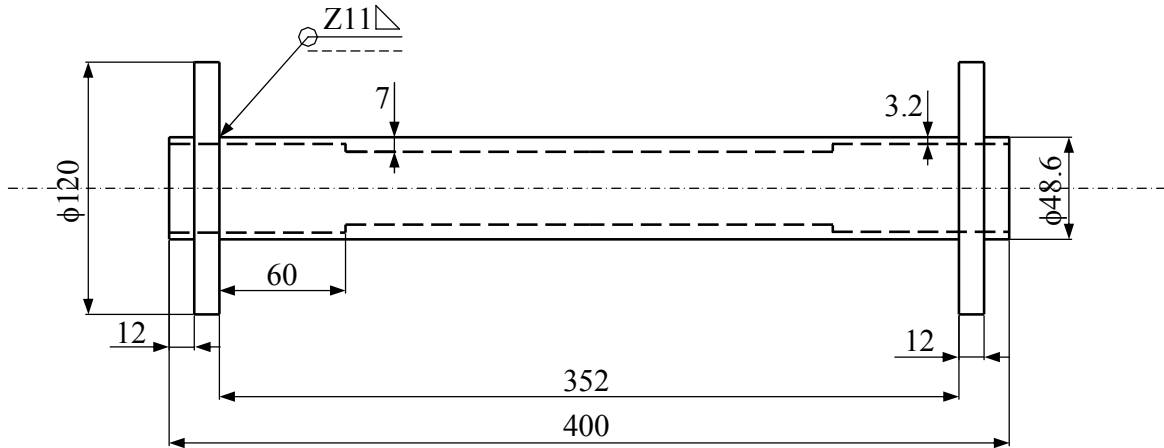


Figure 3: Steel welded joints tested by Razmjoo [20].

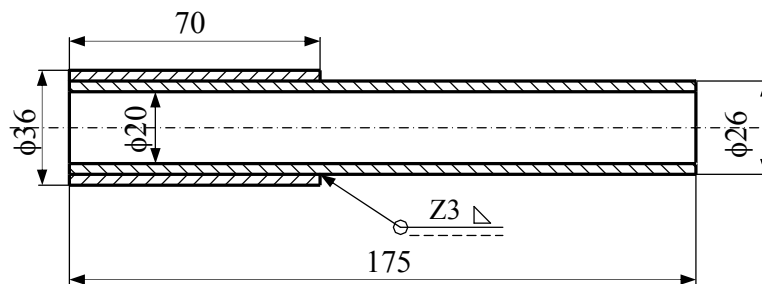


Figure 4: Aluminium welded joints tested by Costa et al. [21].

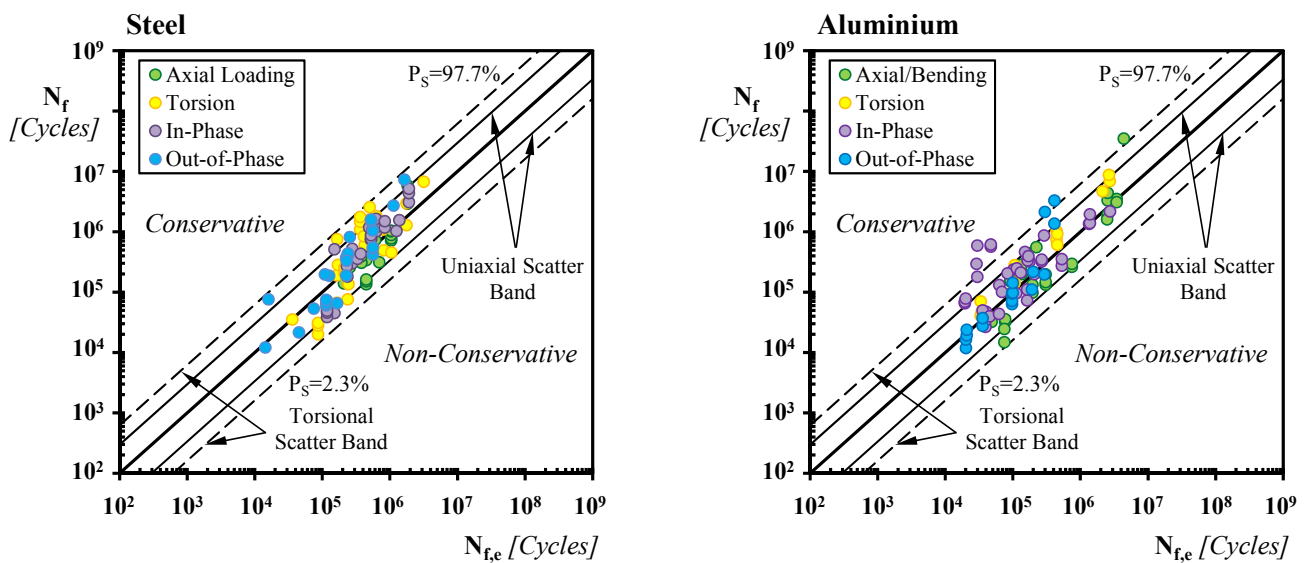


Figure 5: Accuracy of the MWCM applied in terms of nominal stresses in estimating fatigue lifetime of thin welded joints.

The error charts of Fig. 5 make it evident that the MWCM applied in terms of nominal stresses is highly accurate in estimating fatigue lifetime of thin welded joints subjected to in-service multiaxial fatigue loading, the level of accuracy being definitely satisfactory simply because we cannot ask a predictive method to be, from a statistical point of view, more accurate than the experimental information used to calibrate the method itself. As to the appropriate nominal standard fatigue curves to be used to design thin welded details against fatigue, it has to be admitted that choosing the correct curve is never an easy task due to the fact that the available standard codes [1, 2] and recommendations [3] were prepared by reanalysing experimental results generated by mainly testing thick welded joints.

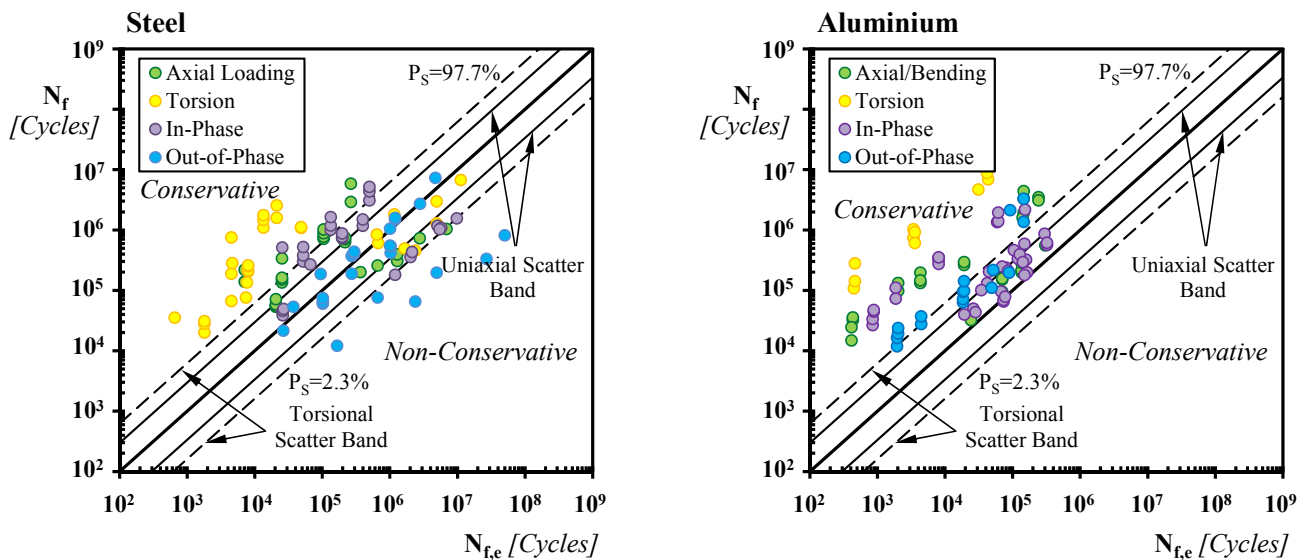


Figure 6: Accuracy of the MWCM applied along with the $r_{ref}=0.05\text{mm}$ concept in estimating fatigue lifetime of thin welded joints.

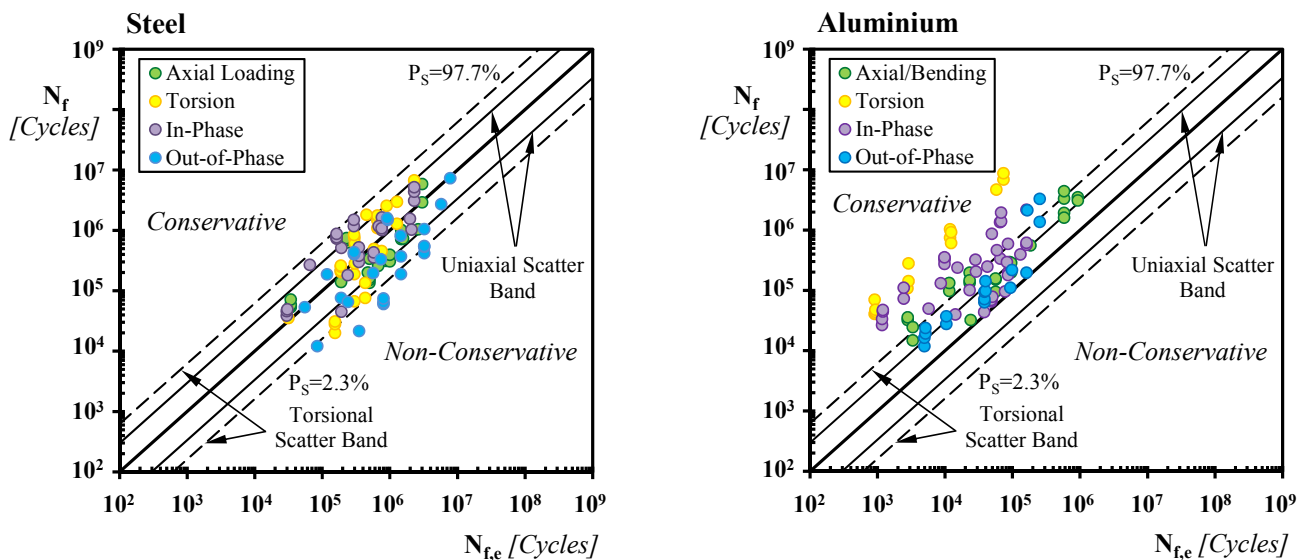


Figure 7: Accuracy of the MWCM applied in conjunction with the Point Method in estimating fatigue lifetime of thin welded joints.

Turning to the accuracy of the MWCM applied along with the reference radius concept, the relevant notch stresses damaging the investigated thin welded joints were determined by solving Finite Element (FE) models done using commercial FE software ANSYS®, the density of the mapped mesh in the process zone being gradually refined until convergence occurred. According to the reference radius approach, the weld toes in the above models were rounded with a fillet having radius equal to 0.05 mm, the schematisation adopted to model the samples tested at LBF being sketched in



Fig. 2b [18, 19]. The overall accuracy of the MWCM applied by rounding the weld toe with a fillet radius of 0.05 mm is summarised in the experimental, N_f , vs. estimated, $N_{f,est}$, fatigue lifetime diagrams reported in Fig. 6, the constants in our criterion's governing equations being determined from the IIW curves [16] recalculated for $P_S=50\%$. The error charts of Fig. 6 suggest that the high level of conservatism characterising the axial and torsional reference curves used to calibrate the MWCM itself led to conservative estimates, the results generated by Razmjoo [20] being, due to an intrinsic fatigue "weakness" depending on the adopted welding technology, the only ones falling in the non-conservative region.

In order to check the accuracy of the MWCM applied in conjunction with the Point Method in estimating multiaxial fatigue lifetime of thin welded joints, the relevant linear-elastic stress fields acting on the process zone of the investigated connections were determined by solving FE models done using commercial code ANSYS®. According to the general rule discussed in Refs [4, 14, 15], the weld toes in the above models were modelled as sharp notches, the schematisation adopted to estimate the reference stress state in the samples tested at LBF being shown in Fig. 2c.

The experimental, N_f , vs. estimated, $N_{f,est}$, number of cycles to failure diagrams of Fig. 6 show that, when calibrated by using the $\Delta\tau_{Ref}$ vs. ρ_w relationships estimated for $P_S=50\%$, the systematic use of our criterion resulted in accurate estimates, the experimental results generated by testing aluminium thin welded joints being characterised by the largest degree of conservatism. The above error chart makes it evident that the obtained level of accuracy is definitively satisfactory: as clearly proven by the error charts of Fig. 6, the MWCM applied along with the PM is seen to be capable of accurately estimating uniaxial/multiaxial fatigue lifetime of both steel and aluminium welded joints, by accurately taking into account not only the scale effect in weldment fatigue, but also the damaging effect associated with the degree of multiaxiality and non-proportionality of the investigated load history.

As to the accuracy shown by the charts of Fig. 6, an interesting aspect which deserves to be mentioned here explicitly is that, whilst in thick welded joints the contribution of cyclic plasticity can be neglected with little loss of accuracy [4], as the thickness of the main plate/tube decreases the role of cyclic plastic deformations becomes more and more important. In spite of the above observations, the MWCM applied along with the PM is seen to be successful also in estimating fatigue damage in very thin welded joints, the relevant stress fields being determined by always forcing the parent material to obey a linear-elastic constitutive law. The above considerations raise the obvious question: why does it work? Although the underlying microstructural mechanisms are based on elasto-plasticity, micro-damage and micro-fracture, it appears to be sufficient to perform a linear elastic analysis and post-process the results. The fact that this simple idea is applicable in so many different situations (see for instance [23]) suggests that this is more than mere coincidence. In order to explain this, the concept of gradient mechanics can be used, in particular the version of gradient elasticity as it has been advocated by Aifantis and co-workers since the early 1990s [24-26]. In this particular enrichment of the standard equations of elasticity, the equilibrium equations are expanded with higher-order spatial derivatives that are the Laplacian of the usual terms, that is:

$$L^T(CLu - \ell^2\nabla^2(Lu)) + b = 0 \quad (26)$$

where L is the usual strain-displacement derivative operator, $\nabla^2 \equiv \nabla^T \cdot \nabla$, C contains the elastic moduli in terms of Young's modulus and Poisson's ratio, b are the body forces and u are the displacements. A new constitutive parameter ℓ is introduced that has the dimension of length and that can be linked to the microstructural properties (such as size of the Representative Volume Element or the inter-particle distance – see [27] for an overview).

Interestingly, Eq. (26) does not have to be solved as a set of fourth-order partial differential equations (p.d.e.). Instead, following the theorems of Ru and Aifantis [26] it is possible to split the equations into two sets of second-order p.d.e., which can be solved *consecutively*. The implications for finite element implementations are that standard element technology can be used [28], whereby firstly the equations of classical elasticity are solved, the solution of which subsequently serves as a source term in a post-processing step that introduces the gradient-dependence into the state variables. That is, there are two important similarities with the TCD methodology: the results of standard linear elasticity are postprocessed, and this postprocessing is governed by a material length scale parameter. This suggests that the two length scales (namely ℓ from gradient mechanics and the critical distance itself from the TCD) have similar meanings and can be related to each other.

The effects of the gradient enrichment in Eq. (26) are that stresses and strains are redistributed over a zone around the stress concentrator (e.g. crack tip or indenter); the size of this redistribution zone is set by ℓ . This is not too different from the TCD-PM technique, whereby representative stresses are sampled at a critical distance away from the stress concentrator. This sheds some light as to why the post-processing of linear elastic results via TCD, or indeed gradient mechanics, is so successful in predicting the lifetime of structural components subjected to fatigue: the post-processing



assumes there is an elastic zone around the stress concentrator in which stresses are redistributed. In reality, the mechanical behaviour in this zone will be governed by micro-structural plasticity, damage and fracture, but the redistribution of the stresses that are the result of such dissipative mechanisms can also conveniently and straightforwardly be described by the TCD or by gradient mechanics – the length scale parameter ℓ of gradient mechanics should then be interpreted as proportional to the size of the plastified (or plastifying) zone around the stress concentrator.

CONCLUSIONS

The MWCM is seen to be successful in estimating multiaxial fatigue lifetime of thin welded joints by directly post-processing the relevant stress state calculated in terms of either nominal stresses or local quantities: this implies that our multiaxial fatigue method can safely be used in situations of practical interest to design welded joints against multiaxial fatigue

REFERENCES

- [1] Anon. Design of steel structures. ENV 1993-1-1, EUROCODE 3.
- [2] Anon. Design of aluminium structures – Part 2: Structures susceptible to fatigue prENV 1999, EUROCODE 9.
- [3] A. Hobbacher, Recommendations for fatigue design of welded joints and components. IIW Document XIII-2151-07/XV-1254-07, May 2007.
- [4] L. Susmel, Multiaxial Notch Fatigue, Woodhead & CRC, Cambridge, UK (2009).
- [5] D. F. Socie, Transactions of the ASME, Journal of Engineering Materials and Technology, 109 (1987) 293.
- [6] L. Susmel, International Journal of Fatigue, 32 (2010) 1875.
- [7] L. Susmel, R. Tovo, Fatigue & Fracture of Engineering Materials & Structures, 27 (2004) 1005.
- [8] L. Susmel, R. Tovo, International Journal of Fatigue, 28 (2006) 564.
- [9] L. Susmel, R. Tovo, P. Lazzarin, International Journal of Fatigue, 27 (2005) 928.
- [10] R. P. Kaufman, T. Topper, In: Biaxial and Multiaxial fatigue and Fracture, Edited by A. Carpinteri, M. de Freitas and A. Spagnoli, Elsevier and ESIS, (2003) 123.
- [11] C. M. Sonsino, International Journal of Fatigue, 29 (2007) 2246.
- [12] L. Susmel, C. M. Sonsino, R. Tovo, International Journal of Fatigue, 33 (2011) 1075.
- [13] L. Susmel, Engineering Failure Analysis, 16 (2009) 1074.
- [14] L. Susmel, International Journal of Fatigue, 30 (2008) 888.
- [15] L. Susmel, International Journal of Fatigue, 31 (2009) 197.
- [16] C. M. Sonsino, Welding in the World 53 ³/₄ (2009) R64.
- [17] L. Susmel, International Journal of Fatigue, 32 (2010) 1057.
- [18] C. M. Sonsino, M. Kueppers, M. Eibl, G. Zhang. International Journal of Fatigue, 28 (2006) 657.
- [19] J. Wiebesiek, K. Störzel, T. Bruder, H. Kaufmann. International Journal of Fatigue, 33 (2011) 992.
- [20] G. R. Razmjoo. TWI, Abington, Cambridge, UK, 1996 (TWI REF. 7309.02/96/909).
- [21] J.D.M. Costa et al., Fatigue & Fracture of Engineering Materials & Structures, 28 (2005) 399.
- [22] E. Haibach, Service Fatigue-Strength – Methods and data for structural analysis. Düsseldorf, Germany, VDI, 1992.
- [23] D. Taylor, The Theory of Critical Distances: a new Perspective in Fracture Mechanics, Elsevier 2007.
- [24] E.C. Aifantis, Int J Engng Sci, 30 (1992) 1279.
- [25] S.B. Altan, E.C. Aifantis, Scripta Metall Mater, 26 (1992) 319.
- [26] C.Q. Ru, E.C. Aifantis, Acta Mech, 101 (1993) 59.
- [27] H. Askes, E.C. Aifantis, Int J Solids Struct, 48 (2011) 1962.
- [28] H. Askes, I. Morata, E. C. Aifantis, Comput Struct, 86 (2008) 1266.